

12. Pham, K. N. *et al.* Multiple glassy states in a simple model system. *Science* **269**, 104–106 (2002).
13. Weeks, E. R., Crocker, J. C., Levitt, A. C., Schofield, A. & Weitz, D. A. Three-dimensional direct imaging of structural relaxation near the colloidal glass transition. *Science* **287**, 627–631 (2000).
14. Pusey, P. N. & van Megen, W. Phase behaviour of concentrated suspensions of nearly hard colloidal spheres. *Nature* **320**, 340–342 (1986).
15. Russel, W. B., Schowalter, W. R. & Saville, D. A. *Colloidal Dispersions* (Cambridge Univ. Press, Cambridge, 1999).
16. Parthasarathy, M. & Klingenberg, D. J. Electrorheology: mechanisms and models. *Mater. Sci. Eng.* **R17**, 57–103 (1996).
17. Tao, R. & Jiang, Q. Simulation of structure formation in an electrorheological fluid. *Phys. Rev. Lett.* **73**, 205–208 (1994).
18. Martin, J. E., Odinek, J. & Halsey, T. C. Evolution of structure in a quiescent electrorheological fluid. *Phys. Rev. Lett.* **69**, 1524–1527 (1992).
19. Martin, J. E., Anderson, R. A. & Tigges, C. P. Simulation of the athermal coarsening of composites structured by a uniaxial field. *J. Chem. Phys.* **108**, 3765–3787 (1998).
20. Dassanayake, U., Fraden, S. & van Blaaderen, A. Structure of electrorheological fluids. *J. Chem. Phys.* **112**, 3851–3858 (2000).
21. Bosma, G. *et al.* Preparation of monodisperse, fluorescent PMMA-latex colloids by dispersion polymerization. *J. Colloid Interf. Sci.* **245**, 292–300 (2002).
22. de Hoog, E. H. A., Kegel, W. K., van Blaaderen, A. & Lekkerkerker, H. N. W. Direct observation of crystallization and aggregation in a phase-separating colloid-polymer suspension. *Phys. Rev. E* **64**, 021407 (2001).
23. Pronk, S. & Frenkel, D. Can stacking faults in hard-sphere crystals anneal out spontaneously? *J. Chem. Phys.* **110**, 4589–4592 (1999).
24. Robbins, M. O., Kremer, K. & Grest, G. S. Phase diagram and dynamics of Yukawa systems. *J. Chem. Phys.* **88**, 3286–3312 (1988).
25. Sirota, E. B. *et al.* Complete phase-diagram of a charged colloidal system - A synchrotron X-ray scattering study. *Phys. Rev. Lett.* **62**, 1524–1527 (1989).
26. Monovoukas, Y. & Gast, A. P. The experimental phase diagram of charged colloidal suspensions. *J. Colloid Interf. Sci.* **128**, 533–548 (1989).
27. El Azhar, F., Baus, M., Ryckaert, J.-P. & Meijer, E. J. Line of triple points for the hard-core Yukawa model: A computer simulation study. **112**, 5121–5126 (2000).
28. Halsey, T. C. & Toor, W. Structure of electrorheological fluids. *Phys. Rev. Lett.* **65**, 2820–2823 (1990).
29. Holtz, J. H. & Asher, S. A. Polymerized colloidal crystal hydrogel films as intelligent chemical sensing materials. *Nature* **389**, 829–832 (1997).
30. O'Brien, R. W. & White, L. R. Electrophoretic mobility of a spherical colloidal particle. *J. Chem. Soc. Faraday Trans. II* **74**, 1607–1626 (1978).

Acknowledgements We thank G. Bosma for particle synthesis, C. van Kats for electrophoresis measurements, H. Wisman for technical support, K. van Walree for the suggestion of TCAB salt, and discussion of charge mechanisms, and J. Hoogenboom, S. Auer and D. Frenkel for discussion. We also thank M. Dijkstra and G. Patey for a critical reading of the manuscript. This work is part of the research program of the 'Stichting voor Fundamenteel Onderzoek der Materie (FOM)', which is financially supported by the 'Nederlandse organisatie voor Wetenschappelijke Onderzoek (NWO)'.

Competing interests statement The authors declare that they have no competing financial interests.

Correspondence and requests for materials should be addressed to A.Y. (e-mail: yethiraj@chem.ubc.ca) or A.v.B. (e-mail: A.vanBlaaderen@phys.uu.nl).

High-temperature superconductor bulk magnets that can trap magnetic fields of over 17 tesla at 29 K

Masaru Tomita*† & Masato Murakami*

* Superconductivity Research Laboratory, Shibaura 1-16-25, Minato-ku, Tokyo 105-0023, Japan

† Railway Technical Research Institute, 2-8-38 Hikari-cho, Kokubunji-shi, Tokyo 185-8540, Japan

Large-grain high-temperature superconductors of the form RE-Ba-Cu-O (where RE is a rare-earth element) can trap magnetic fields of several tesla at low temperatures, and so can be used for permanent magnet applications^{1,2}. The magnitude of the trapped field is proportional to the critical current density and the volume of the superconductor^{3,4}. Various potential engineering applications for such magnets have emerged^{5–13}, and some have already been commercialized^{7–10}. However, the range of applications is limited by poor mechanical stability and low

thermal conductivity of the bulk superconductors^{14–17}; RE-Ba-Cu-O magnets have been found to fracture during high-field activation, owing to magnetic pressure^{14–16}. Here we present a post-fabrication treatment that improves the mechanical properties as well as thermal conductivity of a bulk Y-Ba-Cu-O magnet, thereby increasing its field-trapping capacity. First, resin impregnation and wrapping the materials in carbon fibre improves the mechanical properties. Second, a small hole drilled into the centre of the magnet allows impregnation of Bi-Pb-Sn-Cd alloy into the superconductor and inclusion of an aluminium wire support, which results in a significant enhancement of thermal stability and internal mechanical strength. As a result, 17.24 T could be trapped, without fracturing, in a bulk Y-Ba-Cu-O sample of 2.65 cm diameter at 29 K.

Bulk RE-Ba-Cu-O superconductors have a complex structure, consisting of an REBa₂Cu₃O_y matrix in which are distributed small particles of RE₂BaCuO₅, REBa₂Cu₃O_y materials undergo the tetragonal to orthorhombic transformation, which causes crystal deformation. During this transformation the crystal takes up oxygen, and as a result the *c* axis shrinks, leading to the formation of microcracks perpendicular to this axis¹⁸. In addition, when the RE-Ba-Cu-O precursors melt, oxygen gas is released from the crystal; some of this gas remains in the sample (because of high viscosity), resulting in the formation of microvoids¹⁹. These defects are difficult to elim-

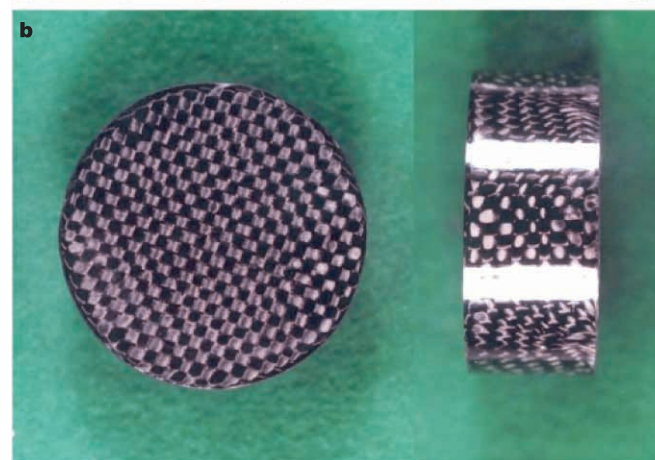
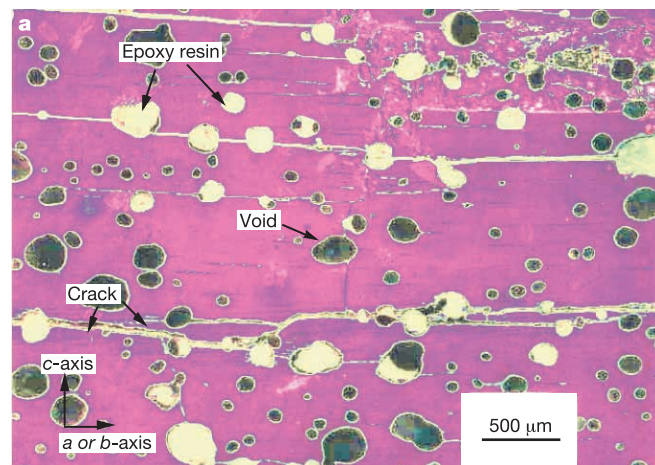


Figure 1 Resin-impregnated Y-Ba-Cu-O with carbon fibre wrapping. **a**, Cross-sectional view of a resin-impregnated Y-Ba-Cu-O (YBCO) disk. Note that resin penetrates through the surface cracks, and fills cracks and voids inside the sample. **b**, A photograph of a YBCO disk wrapped with carbon fibre fabric and resin-impregnated. The stripes of carbon fibres are clearly visible. The carbon fibre reduced the thermal expansion coefficient, and further enhanced the mechanical strength of the resin.

inate, and cause a deterioration of the mechanical properties. Thus the tensile strength of bulk Y-Ba-Cu-O (YBCO) along the *a*-*b* plane is relatively low, ranging from 10 to 30 MPa (ref. 20).

The interaction of the trapped field and the current causes an outward pressure proportional to the trapped field. Therefore, the tensile strength (σ_B) sets the maximum trapped field (B_{\max}), which is to first approximation given by the following equation²¹:

$$\sigma_B = 0.282B_{\max}^2 \quad (1)$$

where σ_B is in MPa, and B_{\max} is in T. According to this relation, the maximum trapped field ranges from 6.0 to 9.4 T in bare bulk superconductors.

Addition of silver has been found effective in improving the mechanical properties, producing a slight increase in the maximum trapped field²². Reinforcement of the sample with metal rings has also been found to be effective in improving the mechanical properties, because the bulk is compressed owing to a difference in thermal contraction^{16,23}. In fact, a trapped field of 14.35 T has been achieved at 22.5 K, although the sample fractured after experiments¹⁶. However, these techniques could not improve the internal mechanical strength or cryo-stability of bulk superconductors.

We have recently found²⁴ that resin can penetrate into a bulk superconductor. When the present sample of YBCO was immersed in molten resin, the resin permeated into the bulk through micro-cracks having openings on the surface (Fig. 1a). The voids connected to these cracks were also filled with resin, which dramatically enhanced the tensile strength from 18.4 to 77.4 MPa (ref. 25). However, a large difference in the thermal expansion coefficient between YBCO ($1 \times 10^{-5} \text{ K}^{-1}$) and resin ($3\text{--}4.5 \times 10^{-5} \text{ K}^{-1}$) caused damage in the surface resin layer during thermal cycles. We therefore wrapped the YBCO disk with carbon fibre fabric before resin impregnation, as carbon fibre has a smaller thermal expansion coefficient of $2 \times 10^{-5} \text{ K}^{-1}$, and can avoid the excessive thermal contraction of the resin.

We measured the trapped field between two resin-impregnated YBCO disks 2.65 cm in diameter and 1.5 cm in thickness, fabricated with the top-seeded melt-growth process²⁶. Each disk was initially characterized by measuring the trapped field profile at 77 K by

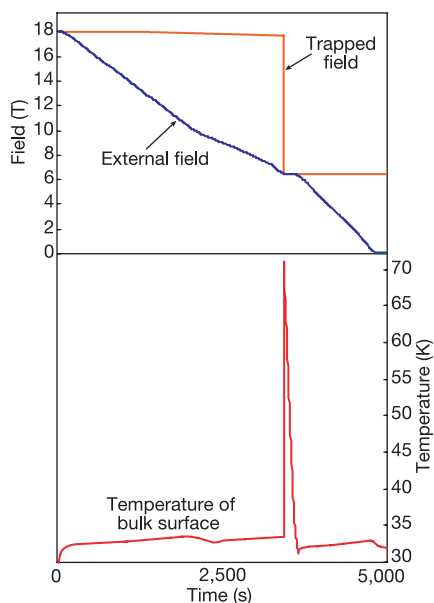


Figure 2 Trapped-field data for two YBCO disks with carbon fibre wrapping and resin impregnation. Shown are the magnetic field between the two disks, the external field, and the temperature of the YBCO disk magnet, as a function of time, when the applied field is decreased from 17.9 T to zero.

cooling the sample with liquid nitrogen in an applied field of 1.5 T (using an normal conducting electromagnet). After removal of the applied field, an axial Hall sensor (model BHA 921, Bell) was scanned over the entire surface, at a constant sensor–surface distance of 1.2 mm. The two disks showed a maximum field of about 0.7 T with a single peak. The YBCO disks were wrapped with carbon fibre fabric, and placed in a plastic mould. Epoxy resin was melted at 70 °C, admitted to the mould, and held for 1 h; outgassing gases were evacuated with a rotary pump. The epoxy resin was composed of phenol-formaldehyde, with polyamine added as hardening material in a weight ratio of 100:32. Finally the mould assembly was heated at 80 °C for 6 h, and at 120 °C for 2 h in air to cure the resin. Figure 1b shows a photograph of a YBCO disk wrapped with carbon fibre fabric and impregnated with resin. The mesh structure of carbon fibre fabrics is visible through the surface resin. No damage occurred in the resin during thermal cycles, thanks to carbon fibre treatment.

For trapped-field measurements, we used an 18-T superconducting hybrid (NbTi and Nb₃Sn) magnet with a bore diameter of 3.6 cm at the Tsukuba Magnet Laboratory of the National Research Institute for Materials. An axial cryogenic Hall sensor (model LHP-MU, AREPOC) was sandwiched by two YBCO disks at their centre to monitor the field. The two disks with the Hall sensor were glued together with GE varnish, and further glued to the cold stage of a variable-temperature cryostat, which allowed us to vary the temperature between 4.2 and 300 K with helium gas circulation. Between two disks, a temperature sensor (model CX-1070 SD, Lake Shore Cernox) was also inserted to monitor the temperature. For each test, the sample was first held at 100 K (that is, above the superconducting transition temperature of YBCO) while the superconducting magnet was energized to a maximum field of 17.9 T. The sample was then cooled to 29 K. The field and temperature of the samples were monitored as the applied field was swept down to zero at a rate of 0.15 T min⁻¹.

Figure 2 shows the measured magnetic field at the centre of the two Y-Ba-Cu-O disks while the field was decreased from 17.9 T to zero. The temperature change of the bulk surface is also shown. Although the temperature of the cryostat was set at 29 K, the temperature of the sample did not reach this value and was 31 K, owing to low thermal conductivity. As the applied field was swept down, the temperature of the sample immediately rose by two degrees and kept increasing. To avoid flux avalanche, we lowered the sweep rate to 0.1 T min⁻¹ when the applied field reached 10 T. The field stayed at 17.9 T at the centre of the sample until the applied field reached 6 T, reflecting an extremely strong flux pinning force. Despite careful control of the field sweeping rate, the temperature of the sample suddenly rose to >70 K at an applied field of 6.0 T and

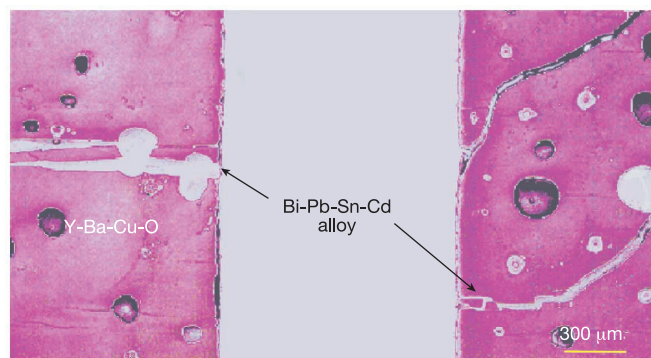


Figure 3 Cross-sectional view of a YBCO disk in which a hole of 1 mm diameter was drilled, followed by Bi-Pb-Sn-Cd alloy impregnation. Note that voids and cracks, along with the hole, are filled with alloy.

the field strength on the bulk surface also dropped from 17.9 to 6.0 T. We then stopped sweeping the field, and monitored the sample temperature. After three minutes the temperature of the sample recovered to 31 K. As the field was decreased further, no temperature spike occurred and the field strength of the bulk surface stayed at 6 T even when the external field reached zero.

After the experiment, the sample was subjected to visual inspection. A large crack was observed on both YBCO disks. We note that a sudden change in field distribution in YBCO disks can be explained in terms of flux jumping; such thermal instability is commonly observed in low-temperature superconductors²⁷. The problem here was that the heat generated in the superconductor could not be effectively transferred to the cooling device. We then performed further similar experiments, but with the sweep rate reduced to $<0.05 \text{ T min}^{-1}$ in a manual mode to allow longer time for heat transfer. We could achieve a trapped field of 14.9 T at 31 K, but the trapped field magnet was unstable and small agitation caused flux jumping. As a result, all the samples were destroyed after high field activation. Similar problems of sample cracking were encountered in previous experiments^{9,14-16}.

The thermal conductivity of bulk YBCO is anisotropic: 3.5 W m K^{-1} along the *c* axis, and 14 W m K^{-1} along the *a-b* plane. We believe that such a low thermal conductivity causes flux jumping. Thus the key to cryo-stability is heat transfer to the cooling device.

In order to overcome this problem, we impregnated the bulk sample with $\text{Bi}_{0.5}\text{-Pb}_{0.27}\text{-Sn}_{0.13}\text{-Cd}_{0.1}$ (Bi-Pb-Sn-Cd) alloy, which has a high thermal conductivity of 200 W m K^{-1} at 29 K. This was achieved with the same method as used for epoxy resin impreg-

nation, as the melting point of this alloy is only 70°C . Another reason for the selection of this alloy was that its thermal expansion coefficient ($2 \times 10^{-5} \text{ K}^{-1}$) is close to that of bulk YBCO, so that thermal stresses could be made negligibly small. This treatment markedly enhanced the thermal conductivity, but flux jump was still unavoidable. This is because the alloy impregnation could enhance the thermal conductivity only at the surface, while the thermal conductivity of the interior region of the disk remained low.

We sought a technique to improve the thermal conductivity inside the sample. To achieve this, we mechanically drilled a hole 1 mm in diameter at the centre of the sample, and followed this by Bi-Pb-Sn-Cd alloy impregnation. This mechanical machining did not degrade the performance of the YBCO disk. Figure 3 is an optical micrograph of the cross-section along the hole for the alloy-impregnated sample. We note that microcracks as well as voids can be filled with Bi-Pb-Sn-Cd alloy through the hole drilled in the sample.

With the aim of full stabilization, we prepared YBCO disk magnets with the following steps. First, two disks were subjected to carbon fibre/resin impregnation with the top and bottom surfaces uncovered. A hole of 1 mm diameter was drilled at the centre of each disk. Then we inserted 0.9-mm-diameter Al wire, of large thermal conductivity ($4,000 \text{ W m K}^{-1}$ at 29 K), into the hole for further enhancement of thermal conductivity. The disks were then placed in a carbon tube, leaving a minimum space around the disk. Bi-Pb-Sn-Cd was melted at 70°C and admitted to the mould.

This configuration was chosen because the surfaces free from the coolant should be thermally insulated to prevent heat leaks. Two YBCO disks were stacked together with GE varnish. This time, six Hall sensors (model LHP-MU, AREPOC) were sandwiched by two YBCO disks to monitor the field distribution at the following locations: the centre, 0.06 cm (two locations), 0.68 cm, 1.01 cm and 1.32 cm away from the centre. This assembly was subjected to trapped field measurements at the sweeping rate of 0.15 T min^{-1} .

Figure 4 shows variation of the field and temperature in the present composite bulk magnet when the applied field was swept

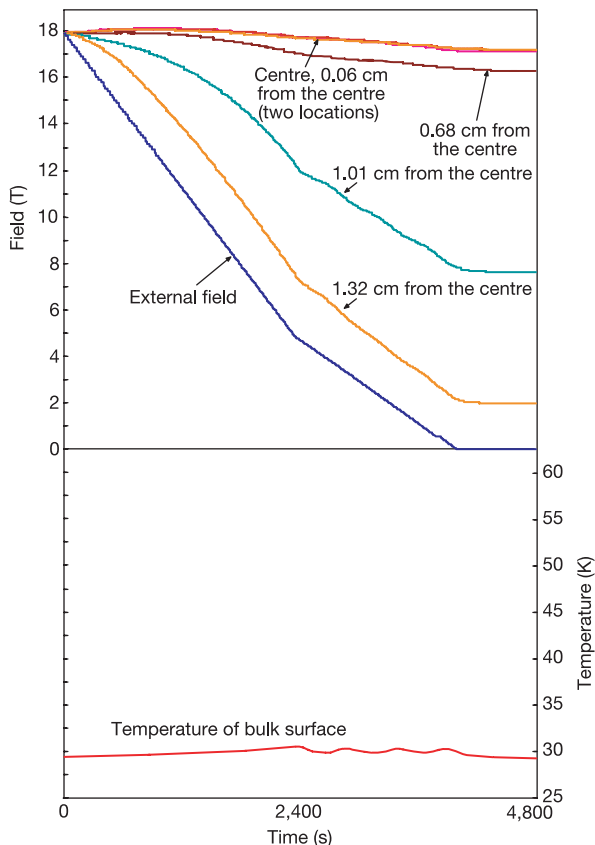


Figure 4 Trapped-field data for two fibre-wrapped, resin-impregnated YBCO disks with embedded Al wire. Shown are the variation of the trapped-field, the external field, and the temperature, for the bulk disks when the external field is reduced from 17.9 T to zero.

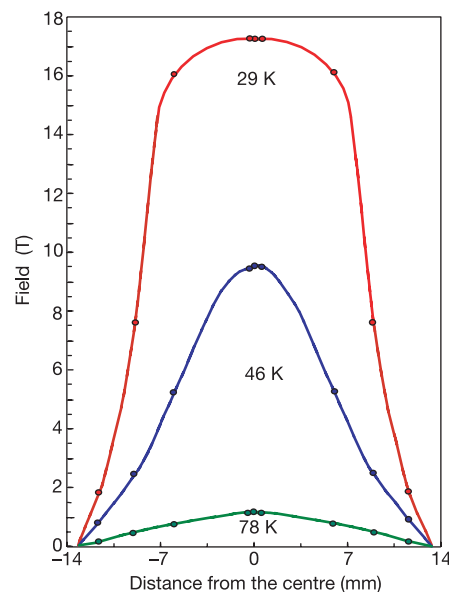


Figure 5 The effect of temperature on trapped-field distribution. The field was trapped between two 26.5-mm-diameter YBCO disks with carbon fibre wrapping, resin impregnation and embedded Al. Data are shown for 29 K, 46 K and 78 K. It is evident that the trapped field is saturated at higher temperatures, but that the field is far below saturation at 29 K, showing that much higher fields could be trapped.

down from 17.90 T to zero. The temperature of the sample reached 29 K, reflecting a marked enhancement of its thermal conductivity. Also, the temperature rise during field sweeping is small compared to the experiment shown in Fig. 2. This also supports the fact that the thermal conductivity was greatly improved in the present configuration. As the applied field is decreased, the field on the superconductor gradually decreased. However, the field at the centre of the sample stayed at an initial value of 17.9 T. No sudden temperature rise occurred during the field-decreasing process, but, because the temperature increased to 30 K at 4 T, we lowered the sweeping rate to provide a safety margin. Even after the external field was removed, a field of >17 T was trapped by the superconductor (Fig. 5). We also performed similar trapped-field experiments at 78 K and 46 K (Fig. 5). The trapped-field profiles at these temperatures show saturation, with a peak field of 9.5 T for 46 K and 1.2 T for 78 K. Compared to the data at 46 and 78 K, the trapped field at 29 K is far below saturation, and hence the present bulk magnet has the potential to trap much higher fields than 17 T if a higher magnetic field is available for activation.

The static field of 17.24 T is attractive for various applications. As long as the sample temperature is kept at 29 K with a cryocooler, a bulk superconductor magnet trapping 17.24 T could be transported to any desired place. This means that a strong static field of 17.24 T limited to the bore space of the superconducting solenoid could be freely used in free space. For magnetic separation of contaminants from polluted water, pre-treatment with ferromagnetic powders is unnecessary for fields larger than 10 T. Therefore, a much simpler separation system could be made. Furthermore, the output of an electromagnetic machine is the product of electric current and magnetic field, so a strong magnetic field is beneficial for the development of high-power, compact machines. The range of a stray field is very small in bulk superconductor magnets, so the deleterious effect of stray field can be localized. We therefore believe that the present results will open the way to new applications of fields from bulk superconducting magnets. □

Received 21 August; accepted 29 November 2002; doi:10.1038/nature01350.

1. Nariki, S., Sakai, N. & Murakami, M. Processing of high-performance Gd-Ba-Cu-O bulk superconductor with Ag addition. *Supercond. Sci. Technol.* **15**, 648–652 (2002).
2. Ikuta, H. *et al.* Melt-processed Sm-Ba-Cu-O superconductors trapping strong magnetic field. *Supercond. Sci. Technol.* **11**, 1345–1347 (1998).
3. Murakami, M. *Melt Processed High Temperature Superconductors* (World Scientific, Singapore, 1991).
4. Cardwell, D. A. Processing and properties of large grain (RE)BCO. *Mater. Sci. Eng. B* **53**, 1–10 (1998).
5. Weinberger, B. R., Lynds, L., Hull, J. R. & Balachandran, U. Low friction in high temperature superconductor bearings. *Appl. Phys. Lett.* **59**, 1132–1134 (1991).
6. Matsunaga, M. *et al.* YBCO bulk for the superconducting bearing for a 10kWh flywheel. *Supercond. Sci. Technol.* **15**, 842–845 (2002).
7. Minami, H. & Yuyama, J. Construction and performance test of a magnetically levitated transport system in vacuum using high- T_c superconductors. *Jpn J. Appl. Phys.* **34**, 346–349 (1995).
8. Kovalev, L. K. *et al.* High output power reluctance electric motors with bulk high-temperature superconductor elements. *Supercond. Sci. Technol.* **15**, 817–822 (2002).
9. Oka, T. *et al.* Construction of 2–5 T class superconducting magnetic field generator with use of an Sm123 bulk superconductor and its application to high-magnetic field demanding devices. *Physica C* **335**, 101–106 (2000).
10. Saho, N., Mizumori, T., Nishijima, N., Murakami, M. & Tomita, M. High- T_c bulk-superconductor based membrane-magnetic separation for water purification. *J. Am. Ceram. Soc.* (in the press).
11. Mizutani, U. *et al.* Application of RE123-bulk superconductors as a permanent magnet in magnetron sputtering film deposition apparatus. *J. Am. Ceram. Soc.* (in the press).
12. Yoo, S. I., Higuchi, T., Sakai, N., Fujimoto, H. & Murakami, M. RE-Ba-Cu-O for high functional superconducting permanent magnet. *Mater. Sci. Eng. B* **52**, 203–210 (1998).
13. Wang, J. *et al.* A scheme of maglev vehicle using high T_c bulk superconductors. *IEEE Trans. Appl. Supercond.* **9**, 904–907 (1999).
14. Ren, Y., Weinstein, R., Liu, J., Sawh, R. P. & Foster, C. Damage caused by magnetic pressure at high trapped field in quasi-permanent magnets composed of melt-textured Y-Ba-Cu-O superconductor. *Physica C* **251**, 15–26 (1995).
15. Gao, L., Xue, Y., Meng, L. & Chu, C. W. Thermal instability, magnetic shielding and trapping in single-grain YBa₂Cu₃O_{7- δ} bulk materials. *Appl. Phys. Lett.* **64**, 520–522 (1994).
16. Fuchs, G. *et al.* Trapped magnetic fields larger than 14 T in bulk YBa₂Cu₃O_{7- δ} . *Appl. Phys. Lett.* **76**, 2107–2109 (2000).
17. Johansen, T. H. Flux-pinning-induced stress and strain in superconductors: Case of a long circular cylinder. *Phys. Rev. B* **60**, 9690–9713 (1999).
18. Diko, P. Thermal stresses and microcracking caused by 211 particles in Y-Ba-Cu-O melt-processed bulks. *Mater. Sci. Eng. B* **53**, 149–153 (1998).

19. Sakai, N., Ishihara, D., Inoue, I. & Murakami, M. Formation of pores in melt-processed RE-Ba-Cu-O and the techniques to reduce pore density. *Supercond. Sci. Technol.* **15**, 698–701 (2002).
20. Sakai, N., Seo, S. J., Inoue, K., Miyamoto, T. & Murakami, M. in *Advances in Superconductivity XI* (eds Koshizuka, N. & Tajima, S.) 685–688 (Springer, Tokyo, 1999).
21. Collings, E. W. & Sumption, M. D. in *Advances in Superconductivity VII* (eds Yamafuji, K. & Morishita, T.) 605–608 (Springer, Tokyo, 1995).
22. Yeh, F. & White, K. W. Fracture toughness behavior of the YBa₂Cu₃O_{7- δ} superconducting ceramic with silver oxide additions. *J. Appl. Phys.* **70**, 4989–4994 (1991).
23. Morita, M. *et al.* Trapped field and mechanical properties of QMG magnet. *Proc. 1988 Int. Workshop on Superconductivity* 115–118 (ISTEC, Tokyo, 1998).
24. Tomita, M. & Murakami, M. Improvement of the mechanical properties of bulk superconductors with resin impregnation. *Supercond. Sci. Technol.* **13**, 722–724 (2000).
25. Tomita, M., Murakami, M. & Katagiri, K. Reliability of mechanical properties for bulk superconductors with resin impregnation. *Physica C* **378–381**, 783–787 (2002).
26. Salama, K. *et al.* Recent developments in melt-textured superconductors. *JOM* 17–28 (June 2000).
27. Iwasa, Y. *Case Studies in Superconducting Magnets* (Plenum, New York, 1994).

Acknowledgements We thank K. Itoh and H. Wada for use of an 18-T superconducting magnet. This work was partially supported by NEDO as Collaborative Research and Development of Fundamental Technologies for Superconductivity Applications.

Competing interests statement The authors declare that they have no competing financial interests.

Correspondence and requests for materials should be addressed to M.T. (e-mail: tomita@rtri.or.jp)

The effects of surfactants on spilling breaking waves

Xinan Liu & James H. Duncan

Department of Mechanical Engineering, University of Maryland, College Park, Maryland 20742, USA

Breaking waves markedly increase the rates of air–sea transfer of momentum, energy and mass^{1–4}. In light to moderate wind conditions, spilling breakers with short wavelengths are observed frequently. Theory and laboratory experiments have shown that, as these waves approach breaking in clean water, a ripple pattern that is dominated by surface tension forms at the crest^{5–14}. Under laboratory conditions and in theory, the transition to turbulent flow is triggered by flow separation under the ripples, typically without leading to overturning of the free surface¹⁵. Water surfaces in nature, however, are typically contaminated by surfactant films that alter the surface tension and produce surface elasticity and viscosity^{16,17}. Here we present the results of laboratory experiments in which spilling breaking waves were generated mechanically in water with a range of surfactant concentrations. We find significant changes in the breaking process owing to surfactants. At the highest concentration of surfactants, a small plunging jet issues from the front face of the wave at a point below the wave crest and entraps a pocket of air on impact with the front face of the wave. The bubbles and turbulence created during this process are likely to increase air–sea transfer.

Experiments were done in a tank of 15 m by 1.2 m with a water depth of 0.8 m. Weak spilling breakers were produced from Froude-scaled mechanically generated dispersively focused wave packets^{18,19} with average frequencies of 1.15, 1.26 and 1.42 Hz. The breaker generation technique and wave-maker motion parameters are identical to those described in ref. 13 (in the present case, the dimensionless wave-maker amplitude is 0.0505). The wave-maker motions are repeatable to within $\pm 0.1\%$ of their amplitude.

All of the experiments reported here were done with a single tank of filtered tap water over a period of 8 d. Rhodamine 6G, a fluorescent dye, was mixed with the water at a concentration of